

Evolution of particle number distribution near roadways. Part III: Traffic analysis and on-road size resolved particulate emission factors

K. Max Zhang^a, Anthony S. Wexler^{a,b,c,*}, Debbie A. Niemeier^b, Yi Fang Zhu^d,
William C. Hinds^d, Constantinos Sioutas^e

^aDepartment of Mechanical and Aeronautical Engineering, University of California, Davis, CA 95616, USA

^bDepartment of Civil and Environmental Engineering, University of California, Davis, CA 95616, USA

^cDepartment of Land, Air, and Water Resources, University of California, Davis, CA 95616, USA

^dDepartment of Environmental Health Sciences, University of California Los Angeles, 650 Charles E. Young Drive South,
Los Angeles, CA 90095, USA

^eDepartment of Civil and Environmental Engineering, University of Southern California, 3620 South Vermont Avenue,
Los Angeles, CA 90089, USA

Received 19 January 2005; received in revised form 28 March 2005; accepted 8 April 2005

Abstract

On-road size-resolved particulate emission factors were computed using concurrently measured carbon monoxide (CO) as a freeway dilution indicator and correlating roadside particle measurements to CO measurements. The emission factors derived for the total particle number agree well with previous on-road investigations. However, this study extends this analysis to produce unique receptor-dependent, size-resolved, road and grid-level emission factor distributions. Both mileage- and fuel-based particle number and mass emission factors at road and grid levels, along with CO emission factors, are presented and the results from freeways with distinctly different percentages of heavy-duty diesel truck traffic are compared. The effects of plume processing on particle number near roadways are shown to be much more profound than on particle mass, further indicating that the adverse health effects observed near roadways are at least partially related to particle numbers.

© 2005 Elsevier Ltd. All rights reserved.

Keywords: Carbon monoxide; Mobile emissions; Traffic; Transportation; Ultrafine particles; Aerosol

1. Introduction

Accurate motor vehicle emission inventories are critical for understanding and controlling air pollution

problems. Vehicle emissions inventories are produced by multiplying emission factors by associated travel activity. While emission factors can be directly measured in the laboratory using dynamometer tests (Rickeard et al., 1996; Graskow et al., 1998; Hall et al., 2000; Hall and Dickens, 2000; Maricq et al., 2002a,b), there is an ongoing debate over whether such tests are able to replicate the real world emissions (Graskow et al., 1998; Hall and Dickens, 2000; Hall et al., 2000; Maricq et al.,

*Corresponding author. Department of Mechanical and Aeronautical Engineering, University of California, Davis, CA 95616, USA. Tel.: +1 530 754 6558; fax: +1 530 752 4158.

E-mail address: aswexler@ucdavis.edu (A.S. Wexler).

2002b). Largely as a result of this debate, in recent years, many researchers pursued a so-called “on-road” approach—deriving emission factors from real-world observations. A brief introduction to four general approaches found in the literature is given here.

Control volume. Hlavinka and Bullin (1988) proposed using a mass balance model to determine emission factors of gaseous pollutants and calculated carbon monoxide (CO) emissions factors using this method. Jamriska and Morawska (2001) adopted a similar approach and extended it to estimating particle number emission factors. Both of these models select a representative portion of the roadway as a control volume, and assume that the two main processes affecting the pollutant concentration—emissions that originate from traffic traveling in the control volume and losses due to airflow carrying the pollutant out of the control volume—are in equilibrium. The effects of sinks, such as gravitational deposition of particles, or of other processes affecting pollutant characteristics are assumed negligible. With controlled ventilation, road tunnels provide a well-defined control volume to study mobile emissions (Abu-Allaban et al., 2002; Gidhagen et al., 2003). The emission factors can then be calculated, in a straightforward manner, from outlet and inlet concentrations, length and cross-sectional area of tunnel, traffic volume and wind speed inside of tunnel.

Correlation with carbon (fuel-based emission factors). Fuel-based pollutant emission factors are generally computed by relating the increase in pollutant concentration to the increase in the total carbon emissions (mostly in forms of carbon dioxide (CO₂) and CO) in a tunnel (e.g. Kirchstetter et al., 1999) or on roads (e.g. Kittelson et al., 2004), which are then in turn related to the carbon content of fuel. The emission factors, expressed as mass of pollutant emitted per unit of fuel consumed, can be combined with fuel sales data to estimate total pollutant emissions (Singer and Harley, 1996). The advantages and drawbacks of this approach were discussed in Sawyer et al. (2000). Assuming vehicle fleet average fuel consumption, distance-based emission factors in particles km⁻¹ can be determined.

Correlation with NO. Janhäll et al. (2004) found that nitric oxide (NO) was a better tracer for traffic related ultrafine particles, than traffic intensity itself after analyzing their measurements of gases (NO, NO_x, SO₂ and O₃) and particles near Göteborg, Sweden. Although NO_x emission rates were not given explicitly in Janhäll et al. (2004), if they are available, the particle emission factor size distribution can be calculated by multiplying their NO-based emission factors by the actual NO emission factors.

Particle dispersion (inverse modeling). Inverse modeling can also be used to determine emission factors (Mulholland and Seinfeld, 1995; Palmgren et al., 1999). Gramotnev et al. (2003) assumed that the total number concentration of particles ranged from ~15 nm to ~1 μm and the average emission factors for vehicles on a road can be approximately described by a Gaussian plume. For example, this type of analysis was used in the Brisbane area, Australia, where CALINE 4 (Benson, 1992) was adapted to obtain the emission factors near a busy road (Gramotnev et al., 2003).

For the remainder of this paper, we will refer to the methods discussed above as control volume, particle-carbon, particle-NO and particle dispersion, respectively. The values of emission factors derived from studies using each of those methods are listed in Table 5. Particulate pollutants’ physico-chemical properties and health effects are closely associated with their size, therefore ideally particle emission factors should be size-resolved. Note only those results from Janhäll et al. (2004) were size resolved, however, the emission rate was implicitly defined (i.e., in terms of particles per ppb NO).

Since evolution of particle distributions is a dynamic process (Zhang et al., 2004), size-resolved particle emission factors (or particle emission factor distributions) are also receptor dependent. In our previous study, we have shown this dynamic process can be divided into two stages, i.e., ‘tailpipe-to-road’ and ‘road-to-ambient’, based on their distinct dilution natures (Zhang and Wexler, 2004). Accordingly, there are three major types of emission factors: tailpipe-level EF, road-level (or curb-level) EF and grid-level EF as described in Table 1. Typical urban and regional air quality models usually employ grid-level EFs as their inputs, while ‘plume-in-grid’ models require tailpipe or road-level EFs. In the field of highway design and planning, information on both road-level and grid-level EFs are necessary to evaluate the impacts of highway traffic on the exposure of commuters, pedestrians and nearby communities. However, none of previous studies have clearly distinguished those EFs.

Table 1
Three major types of emission factors and their descriptions

EF	Description
Tailpipe-level	The emission profiles near the exit of the tailpipe
Road-level	The emission profiles on or near the roadway curb
Grid-level	The emission profiles near the end of plume processing (particle dynamics slows down significantly at this point)

This paper represents the third part of our investigation of plume-processing of mobile emissions (Zhang and Wexler, 2004; Zhang et al., 2004). The objective of this study is to introduce and implement a method to derive on-road size resolved particle emission factors. We have chosen to use the inverse modeling approach. However, considering the dynamic nature of particles near roadways (Zhang et al., 2004), rather than focusing on particle number directly, we first determine CO emission factors by inverse modeling its dispersion near freeways; we then relate CO emission factors to the concurrently measured particle data. Thus, we are able to present the size distributions of particle emission factors at road and grid levels. We begin this paper with a description of the basic theory and demonstrate the applicability of the proposed method. We then turn to a discussion of the traffic analysis procedures and a short introduction to the two dispersion models we employed. Finally, both distance- and fuel-based particle number and mass emission factors at road and grid levels are presented.

2. Theory and methodology

Palmgren et al. (1999) proposed to calculate emission factors by inverse modeling when the chemical transformations can be disregarded. We transform the original equation as

$$q_h = \frac{C_h - C_{h,\text{background}}}{F_h N_h / V_h}. \quad (1)$$

In Eq. (1) the index h refers to a particular hour of the day; q_h (pollutant vehicle⁻¹ km⁻¹) is the emission factor; C_h and $C_{h,\text{background}}$ (pollutant m⁻³) are the receptor concentration and background or upwind concentrations, respectively; N_h is traffic volume (vehicle h⁻¹) and V_h is the average traffic speed (km h⁻¹); F_h (m⁻³) accounts for dilution and deposition. Apart from the caveats reported in Palmgren et al. (1999), we would like to point out that (1) F_h not only depends on meteorology as originally suggested, but also depends on roadway geometry or street canyon configuration; (2) F_h is receptor-dependent, the implications of which are discussed later in this section; and finally (3) F_h is in theory species-dependent because different species have different deposition loss rates.

Here we posit that F_h derived by a non-reactive gas such as CO equally applies to particles when (1) deposition of both the gas and particles can be neglected and (2) the concentrations of the non-reactive gas concentrations selected for inverse modeling are significantly above background/upwind levels. These two premises ensure that F_h solely represents dilution, and we will denote F_h as the dilution factor. A discussion of the validity of these premises follows.

The deposition velocity for CO is usually <0.1 cm s⁻¹. For an inversion height of 100 m, a rather conservative estimation, the characteristic time scale for CO deposition is over 10⁵ s, much larger than the evolution time scale, usually around 200–300 s (Zhang and Wexler, 2004). Within this time scale of evolution, the behavior of ultrafine particles resembles that of the gas. For a particle with 100 nm diameter, its characteristic relaxation time is about 10⁻⁷ s and its deposition time scale is over 10³ s, which implies that those particles always follow streamlines and their deposition loss can also be neglected. The dilution factor derived assuming an inert gas pollutant then equally applies to the dilution of particle number and CO. Nevertheless, particles differ from CO in that during dilution their size (and composition) may change due to condensation and evaporation.

Current measurement techniques are not able to capture the entire particle size distribution spectrum. The total number of a particle size bounded control volume is not conserved due to the dynamics of the small particles (Zhang et al., 2004). We showed that a large number of particles grew into the >10 nm range around 30–90 m downwind of the freeways; beyond 90 m, some shrink to <10 nm range and some continued growing to >100 nm as result of competition between partial pressure and vapor pressure (Zhang et al., 2004). Thus extra caution is needed in directly simulating particle number dispersion.

The approach taken in this study is described as follows: we first utilize two highway dispersion models to simulate CO concentrations at downwind distances where the concentrations were substantially above upwind levels. Then those CO emission factors best fitting the measured data were identified. Receptor-dependent dilution factors were obtained using Eq. (1). Since for a specific road at a particular time, N_h and V_h are the same for gas and particles, we can derive a practical coefficient D accounting for both dilution and traffic:

$$D = \frac{q_h^{\text{CO}}}{C_h^{\text{CO}} - C_{h,\text{background}}^{\text{CO}}},$$

$$q_h^{\text{particle}} = D \left(C_h^{\text{particle}} - C_{h,\text{background}}^{\text{particle}} \right). \quad (2)$$

Finally, we transform particle number-concentration size distributions to particle emission-factor size distributions using Eq. (2). Note that measured upwind CO concentrations were taken as background.

3. Field measurements and traffic analysis

In addition to particle number concentrations and size distributions in the size range from 6 to 220 nm, CO, and

black carbon concentrations as well as meteorological data measured at various upwind/downwind distances, we also measured traffic near two major freeways in Los Angeles, CA, 405 and 710, in both summer and winter seasons (Zhu et al., 2002a, b). To be consistent with our previous work, we refer to roadway segments as 405S (i.e., summer study near Highway 405), 405W, 710S and

710W. The road geometry and meteorological parameters, used as inputs for the dispersion model, are summarized in Table 2. Additional information can be found in Zhu et al. (2002a, b).

To estimate traffic volumes, we conducted a comprehensive traffic analyses of videos recorded during the field studies. To avoid repetition, we use only 405S as an example to describe the analysis procedure. Traffic volumes were recorded by video for six hours during June 21, 2001 at the I-405 sampling site. The video records were counted three times at two-minute intervals. For the northbound traffic, we were able to count traffic volumes using four standard vehicle classes, namely, passenger cars, vans, small trucks and large trucks. However, only non-trucks and trucks could be reasonably distinguished for the southbound traffic.

To calculate vehicle speeds, which are necessary for computing emission factors, we timed 13 randomly selected vehicles every two minutes passing the width of a reference location. The recording position and angle prevented us from measuring the speed in the

Table 2
Road conditions and meteorological parameters collected during the field campaign

Road and meteo. parameters	405S	405W	710S	710W
Road elevation (m)	4.5		0.0	
Road width (m)	30		26	
Wind direction (°)	225	225	200	200
Wind deviation (°)	23	23	45	45
Wind speed (m s^{-1})	1.5	1.4	1.3	1.2
Temperature (°C)	29–35	18–30	31–35	18–30

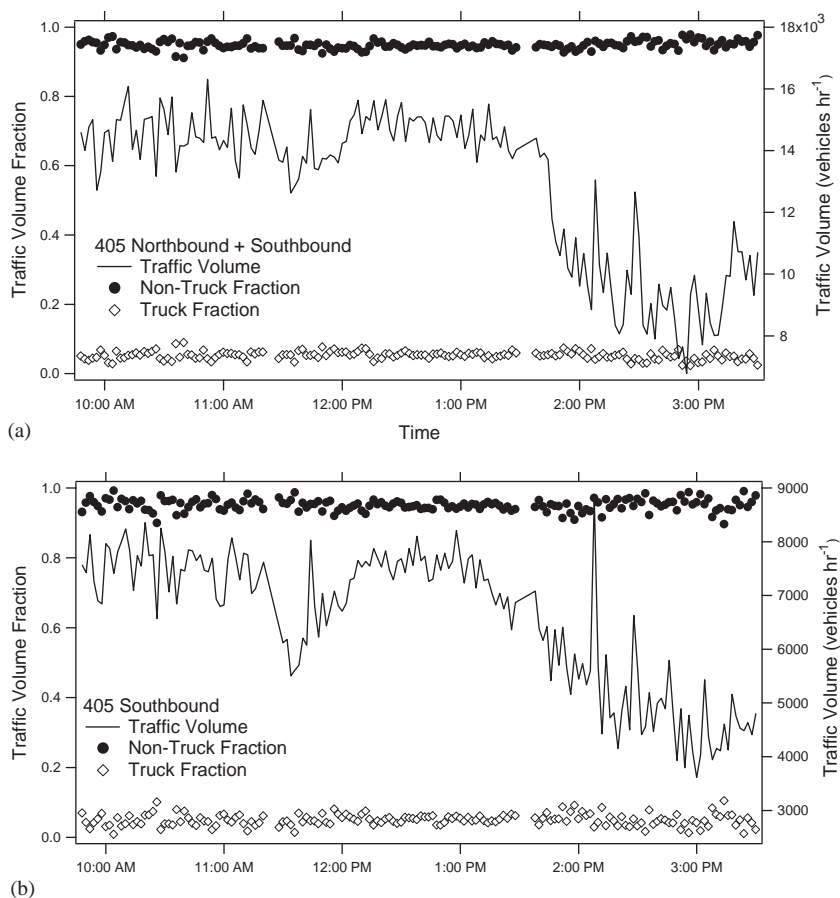


Fig. 1. Traffic mix and volumes in Highway 405 summer study for (a) Northbound and Southbound, (b) Southbound, (c) Northbound and (d) Northbound vehicle class resolved.

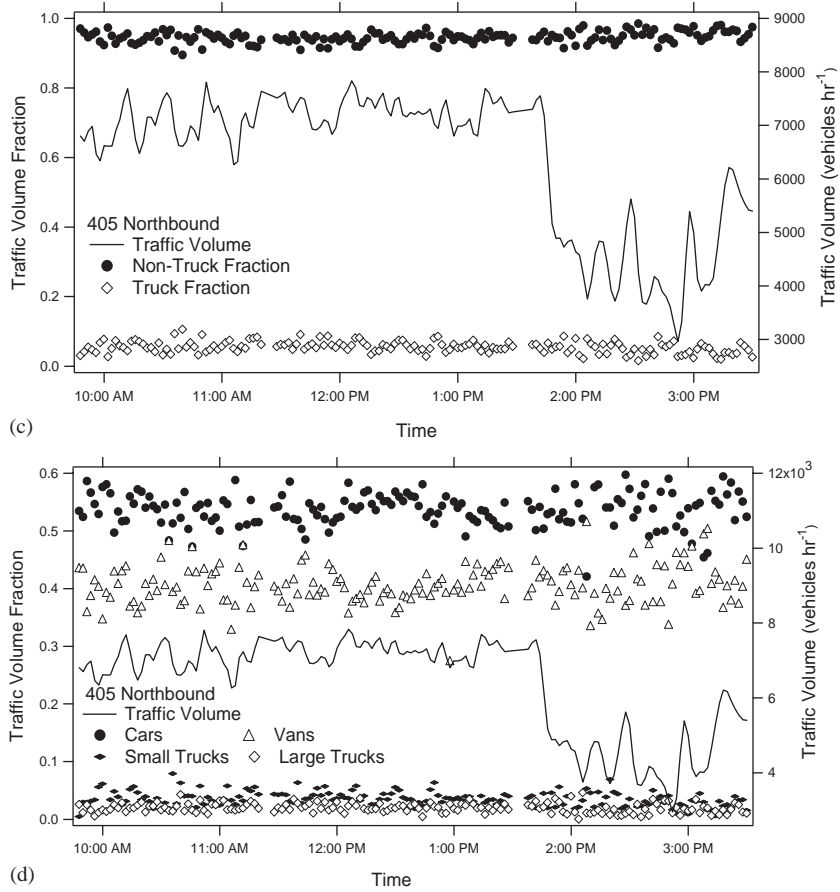


Fig. 1. (Continued)

Table 3
Summary of traffic analysis (mean ± standard deviation)

	405S			405W ^a	710S
	Total	Uncongested	Congested		
Traffic volume (vehicle h ⁻¹)	12900 ± 2500	14490 ± 760	9600 ± 1400	15290 ± 770	12540 ± 680
Truck fraction (%)	5.2% ± 1.2%	5.4% ± 1.1%	4.8% ± 1.3%	5.3% ± 1.0%	23.2% ± 3.3%
Non-truck fraction (%)	94.8% ± 1.2%	94.6% ± 1.1%	95.2% ± 1.3%	94.7% ± 1.0%	76.8% ± 3.3%
Average speed (mile h ⁻¹)	N/A	52.3 ± 0.33	9.8 ± 0.4	N/A	N/A

^auncongested condition

Southbound lane directly. We then calculated a volume–speed curve using our observations from the closest four lanes to project speeds for the lanes furthest out (opposite bound vehicles) based on traffic counts for those lanes. Fig. 1 and Table 3 show the final results of this part of our analysis.

Non-trucks dominated the vehicle mix on Highway 405. The averages of the fractions of non-trucks in the Northbound and Southbound directions overall stayed

within a narrow range from 0.94 to 0.95. Among non-trucks, the fractions of passenger cars and vans were generally steady with over 30% more cars than vans in the Northbound direction. Traffic volumes were classified into uncongested and congested conditions. The congested traffic volume was about 35% less than the uncongested, and occurred about an hour earlier than in the Northbound direction. Seasonal differences on Highway 405 traffic were not appreciable; 405W showed

a similar vehicle mix, but around 10% higher traffic volume in the winter season.

Due to some technical problems in their recording, 710S and 710W videos turned out to be very challenging for analysis. It is also worth noting that the 710 vehicle mix is influenced by on-road trucks that are mostly likely linked to port activities in Long Beach, CA. Our analysis on 710S traffic, summarized in Table 3, may therefore not be representative of general freeway conditions.

4. Dispersion models

We employed two highway-oriented dispersion models to determine emission factors: CALINE 4 (Benson, 1992), developed by California Department of Transportation, and UCD 2001 (Held et al., 2003), developed by scientists at University of California, Davis. A brief introduction of both models is presented below.

4.1. CALINE 4

The CALINE 3/4 models (Benson, 1992) divide the roadway segments into a series of elements from which incremental concentrations are computed and summed. Each element is modeled as an “equivalent” finite line sources (FLS). Incremental downwind concentrations are computed using crosswind Gaussian formulation for a line source of finite strength.

CALINE treats the region directly above the roadway as a zone of uniform emissions and turbulence called a “mixing zone” (Benson, 1992). The primary use of the mixing zone is to establish initial Gaussian dispersion parameters at a reference distance near the edge of a roadway. The CALINE dispersion parameterizations are based in part on roadway geometry and wind direction. Downwind of the roadway edge, the CALINE models determine the Gaussian dispersion parameters with modified Pasquill–Turner curves to account for the effects of vehicle-induced thermal turbulence (Benson, 1992).

4.2. UCD 2001

The UCD 2001 model (Held et al., 2003) is based on a simplified dispersion algorithm rather than a K-theory or higher-order closure approach (Stull, 1988). It uses a steady state solution to the SEADE (Huang, 1979) for a continuous point source which accounts for shear in the vertical wind profile and variation of eddy diffusivity with elevation. The Huang solution assumes that the concentration distribution in the crosswind direction is Gaussian (Huang, 1979), but the vertical concentration distribution is considerably more complex and is dependent upon a modified Bessel function.

The UCD model is based on a three-dimensional array of point sources rather than the two-dimensional

line source used in the CALINE models. Since a point source does not have to be aligned with the wind in a special way, it eliminates the arbitrary FLS rotation that is necessary in the CALINE approach. Similar to CALINE models, UCD 2001 assumes all emissions emanate from a mixing zone above the roadway (Held et al., 2003).

5. Results and discussion

5.1. On-road CO emission factors

The optimal CO emission factors were acquired by minimizing the root mean square (RMS) differences between modeled and measured concentrations at selected distances. Since the applicable limits of both CALINE4 and UCD 2001 are about 100 m from the centerline of the roadway, only that field data collected within 100 m was used in the minimization, i.e., 30, 60 and 90 m for 405S and 405W; 17, 20, 30, 60, 90 m for 710S and 710W. The results are illustrated in Fig. 2 and summarized in Table 4.

The optimal CO emission factors are well within the range of the previously reported values (Held et al., 2001; Kean et al., 2003; McGaughey et al., 2004). The two sets of emission factors, i.e., from CALINE4 and UCD 2001, respectively, differ by <6% for 405S/W and <13% for 710S/W. UCD 2001 predictions match the measurement data closer than CALINE4 based on RMS metrics except for 405W, where the reverse is true. Nevertheless, considering that the two models operate with different principles, the closely matching results suggest that we can be reasonably confident using the derived on-road CO emission factor estimates.

It is worth noting that although we did not use 150 m data in the minimization, both modeled results actually fall within the error range of the observed data at 150 m, indicating the dispersion models may well be applicable in this range as well. Because of this, we also elected to use the proposed method to obtain particle emission factor distributions at 150 m. Due to lack of measurements, these estimates do not take into account possible aerosol dynamics between 150 m and the 1 km scale grid that would be employed in an Eulerian model. However, since the dynamics beyond this distance has slowed down considerably (Zhang and Wexler, 2004), these emission factor distributions are our best estimate for grid level emissions.

5.2. On-road particle number emission factors

5.2.1. Distance-based emission factor

A clear advantage of distance-based emission factors is that they are directly applicable for the purposes of estimating emissions for highway planning and

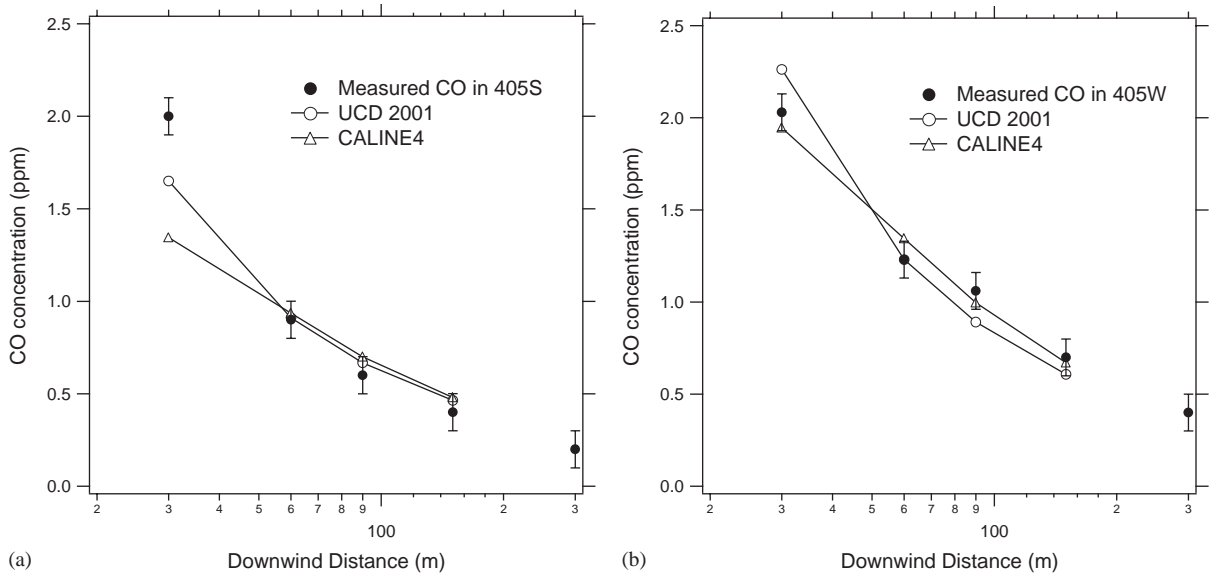


Fig. 2. Measured and predicted carbon monoxide concentrations in (a) Highway 405 summer and (b) Highway 405 winter studies.

Table 4

On-road carbon monoxide emission factors predicted by the two highway dispersion models, CALINE4 and UCD 2001

	CALINE4		UCD 2001	
	EF ^a	RMS	EF ^a	RMS
405S	5.3	0.21	5.6	0.12
405W	7.9	0.07	7.8	0.11
710S	6.2	0.26	5.5	0.075
710W	5.8	0.25	5.1	0.062

^aunit is g mile⁻¹ vehicle⁻¹.

construction. Fig. 3 depicts the distanced-based emission factor size distributions from 405S, 405W, 710S and 710W. For the measurements near Highway 405 at 30 m, the actual sampling location was only 15 m from the curb side; for the measurements near Highway 710 at 17 m, the actual sampling location was 4 m from the curb side. So their corresponding distributions represent our best estimate for the emissions at road level. As discussed earlier, the distributions at 150 m represent the emissions at the grid level. The error bars in Fig. 4 take into account the uncertainties in the CO emission factors, $\sigma_{EF,CO}$, in the CO concentration measurements, σ_{CO} , and in the particle size distribution measurements, σ_p^i . The uncertainties associated with traffic measurement have already been incorporated into $\sigma_{EF,CO}$. σ_{CO} is taken to be 0.1 ppm, the detection limit of the CO measuring instrument (Dasibi Model 3008, Environmental Corp.), which has already been reflected in

Fig. 2. Variance in the CO measurement due to turbulence was neglected because the 15 min averaging time is assumed to represent the ensemble average. So the overall uncertainty for the emission factor for a size bin i , $\sigma_{EF,P}^i$, is

$$\frac{\sigma_{EF,P}^i}{EF_P^i} = \sqrt{\left(\frac{\sigma_{EF,CO}}{EF_{CO}}\right)^2 + \left(\frac{\sigma_{CO}}{C_{CO}}\right)^2 + \left(\frac{\sigma_p^i}{C_p^i}\right)^2}. \quad (3)$$

The scarcity of size-resolved particle emission factor distributions reported in the literature makes it impractical to make peer-comparison between our results and others. In contrast, there have been numerous on-road studies yielding emission factors in terms of total particle number in certain size ranges. Table 5 compares the total number emission factors from various studies including the current work. Despite the appreciable range of geographical location and traffic volume, the emission factors from different studies agree well with each other in the range of 10^{13} – 10^{14} particles km⁻¹ vehicle⁻¹. The lower limit of emission factor from this study is similar to that from gasoline engines derived by Kirchstetter et al. (1999) in the Caldecott tunnel, California. This comparison partially validates the proposed method.

Road-level emissions in the summer season are generally multi-modal, while grid-level emissions are distinctly mono-modal. The large differences in emission profiles from road to grid-level, especially in 405S and 710S, are a clear indication of plume processing of mobile emissions. The particle dynamics from road to ambient can be largely explained by the interaction of

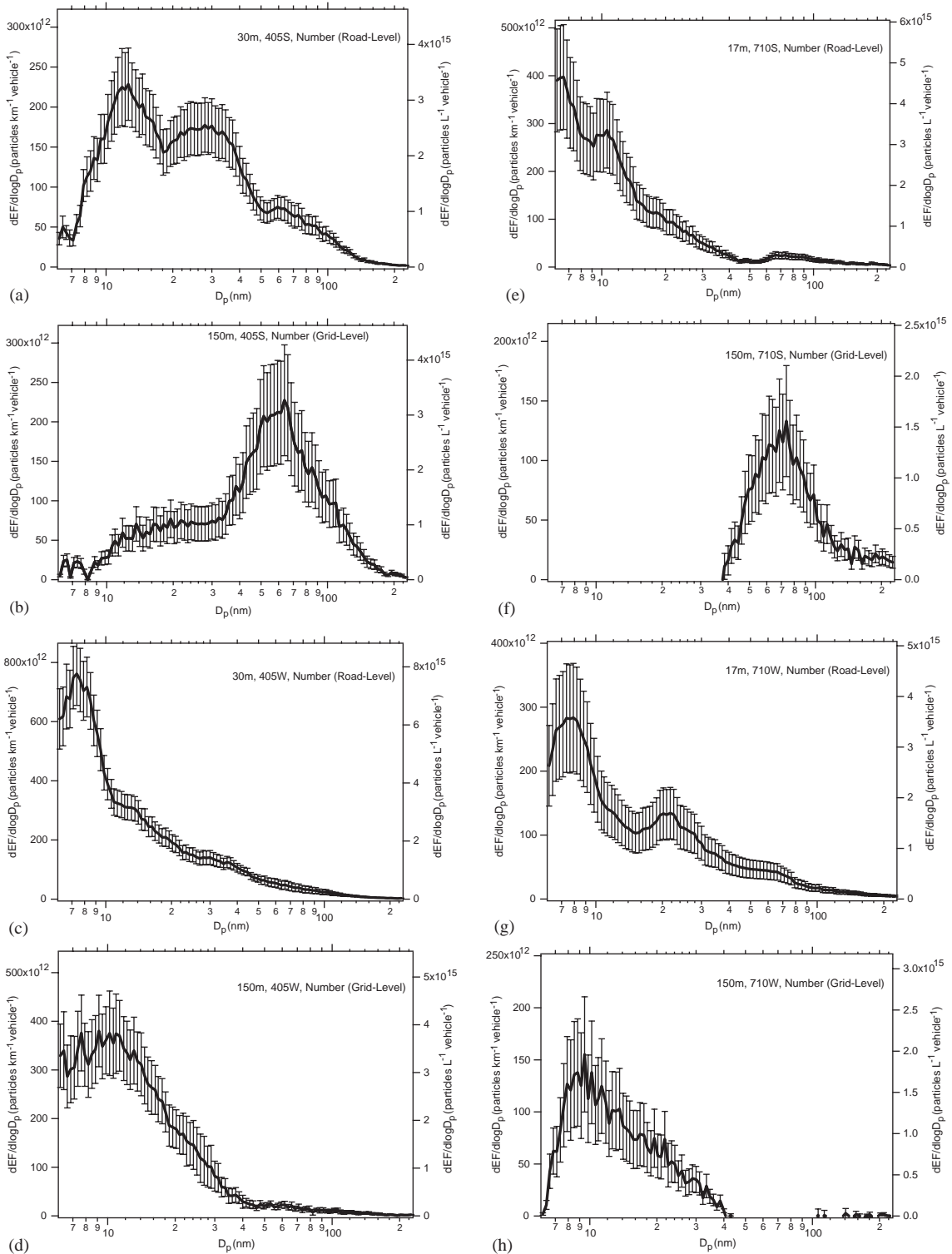


Fig. 3. Distance (left axis) and fuel-based (right axis) particle number emission factors in Highway 405 summer and winter studies. The error bars only denote those of distanced-based emission factors. Zero EF values indicate measured concentration below the background level.

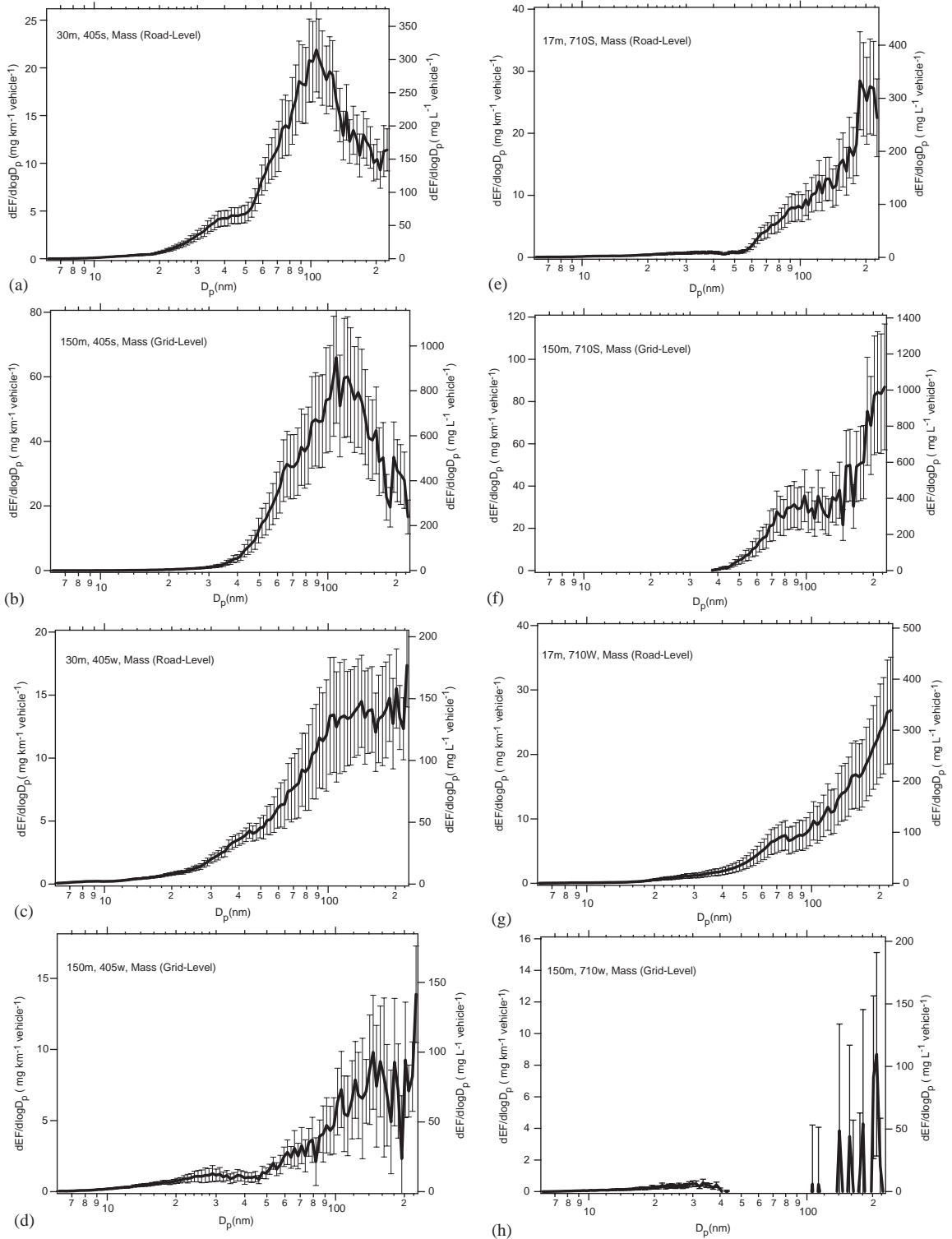


Fig. 4. Distance (left axis) and fuel-based (right axis) particle mass emission factors in Highway 405 summer and winter studies. The error bars only denote those of distanced-based emission factors. Zero EF values indicate measured concentration below the background level.

Table 5
Comparison of particle number emission factors from various on-road studies

Methods	EF (particles vehicles ⁻¹ km ⁻¹)	Size range (nm)	Traffic volume (vehicles h ⁻¹)	Source	Location	Vehicle mix
Control volume	1.75 × 10 ¹⁴	5–900	3960–5040	Jamriska and Morawska (2001)	Brisbane, Australia	6% diesel
	5.44 × 10 ¹³ –3.13 × 10 ¹⁴	10–400	293–814	Abu-Allaban et al. (2002)	Tuscarora Mountain Tunnel, Pennsylvania	47.1–85.5% HD ^c
Particle-C	4.1 × 10 ¹³ (G) ^a –2.5 × 10 ¹⁶ (D) ^b	> 10	2191–4214	Kirchstetter et al. (1999)	Caldecott Tunnel, California	3.7–4.8% HD for bore 1; 0.29–0.36% HD for bore 2
	1.9 × 10 ¹³ –9.9 × 10 ¹⁴	3–1000	N/A	Kittelson et al. (2004)	The Twin Cities Area, Minnesota	N/A
Particle-NO	268 particle cm ⁻³ per ppb NO	10–368	44–648	Janhäll et al. (2004)	Göteborg, Sweden	N/A
Particle dispersion	2.1 × 10 ¹⁴ –4.0 × 10 ¹⁴	15–700	2928–3504	Gramotnev et al. (2003)	Brisbane, Australia	N/A
	9.6 × 10 ¹³ –4.7 × 10 ^{14c}	6–220	14,010–15,290	This study	Los Angeles, California	5.5% truck

^aFor gasoline engine powered vehicles. Note that these values were misreported in Zhang and Wexler (2002).

^bFor diesel engine powered vehicles. Note that these values were misreported in Zhang and Wexler (2002).

^cHighway 405 summer and winter studies only.

dilution and condensation/evaporation of volatile and semi-volatile materials in the exhaust composition as has been discussed in details by Zhang et al. (2004).

Highway 710 has substantially higher diesel truck fractions (Table 3). Unfortunately, due to the technical difficulties in the 710 videos, we could not separate out the contributions from gasoline and diesel-powered vehicles quantitatively. However, some insight can be gained by comparing the counterpart measurements for Highway 405 and 710. Despite different diesel truck fractions, the shapes and magnitudes of grid-level emissions for Highway 405 and 710 are remarkably similar with conspicuous seasonal effects. For the summer season, both grid-level emissions are mainly composed of a single mode around 40–100 nm (Fig. 3(b) and (f)); while for the winter, the common single mode shift to a much smaller size, around 10–20 nm (Fig. 3(d) and (h)).

Although we expected Highway 710 would have higher emission rates because several studies showed that diesel trucks usually have much higher emission rates than gasoline-powered vehicles (Kirchstetter et al. (1999)), our estimation of the particle emission rates for Highway 405 and 710 at grid level are quite similar considering the uncertainties. One possible explanation is that the majority of diesel emissions are volatile, which tend to evaporate during the plume processing, i.e., from road to grid level.

5.2.2. Fuel-based emission factor

Since CO₂ concentrations were not measured in the field studies, we were unable to derive fuel-based CO emission factors directly (the procedure to derive fuel-based emission factors were briefly discussed in the Introduction). As a reasonable alternative, we relied on published work for the appropriate values. Two of the most recent studies conducted in Southern and Northern California, respectively, Singer and Harley (2000) and Kean et al. (2003), give very different CO emission factors, i.e. 80 and 40 g L⁻¹, respectively. The former takes into account income status and other factors. The latter appears to be consistent with most other studies. We choose a value of 50 with 10 g L⁻¹ uncertainties for 405S and 405W, and 40 g L⁻¹ for 710S and 710W.

The shapes of the fuel-based distributions are essentially the same as the distance-based ones, so we depict them in the same figures (but with different axes). The relative errors are slightly different as the first term in the square root of Eq. (3) arises from the relative errors of fuel-based CO emission factors. The error bars in Figs. 3 and 4 denote only those of distanced-based emission factors.

5.3. On-road ultrafine particle mass emission factors

Simply assuming a spherical shape and uniform density (1.0 g cm⁻³), we can tentatively present the

distributions in particle mass (Fig. 4). However, due to the existence of particle aggregates and varying particle density with size (Park et al., 2003), these results are likely to be more uncertain than particle number emission factors. Even with the potential uncertainties, the differences between the shapes of particle number and mass emission factor distributions are significant. The mass emission factor distributions are in general mono-modal, and have no appreciable size shift from road (at 17 m or 30 m) to grid-level emissions (at 150 m), a result of the third-moment distribution leaning towards larger particles sizes. The deep contrasts indicate that the effects of plume processing on particle number are much more profound than on particle mass, which further suggests that adverse health effects observed near roadways (Kunzli et al., 2003) are at least partially related to particle numbers.

Since we have measurements at 150 m for both Highway 405 and 710 in the summer and the corresponding traffic mix has been determined (Table 3), we are able to evaluate the mass emission rates for two main classes of vehicles, i.e., trucks and non-trucks. However, because emission factor distributions shown in Fig. 4 have been truncated, we fit the distribution by log-normal functions to extrapolate the concentrations beyond the measurement range (<220 nm). The underlying assumption is that no additional modes are beyond this measurement range. We take a simplified approach as follows:

$$\begin{aligned} E_{NT}f_{NT,405} + E_Tf_{T,405} &= E_{405}, \\ E_{NT}f_{NT,710} + E_Tf_{T,710} &= E_{710}, \end{aligned} \quad (4)$$

where E_T and E_{NT} (unit: $\text{mg km}^{-1} \text{vehicle}^{-1}$) are the truck and non-truck emission rates, respectively; f_T and f_{NT} are the traffic fraction of trucks and non-trucks; E_{405} and E_{710} are the total emission rates (unit: $\text{mg km}^{-1} \text{vehicle}^{-1}$) for Highway 405 and 710, respectively. By applying the corresponding values, we acquire E_T and E_{NT} to be around 133 and $21 \text{ mg km}^{-1} \text{vehicle}^{-1}$, respectively, for fine-mode particle sizes. These emission rates, albeit preliminary, are consistent with previous studies (Cadle et al., 2001; Maricq et al., 2002a, b). However, the non-truck emission rate is in the high end of the reported values.

6. Conclusion

In this study, we present new receptor-dependent, road and grid-level particulate emissions in size-resolved emission factor distributions near the roadway and at the 1 km distance scale, which were obtained by inverse-modeling a chemically inert, concurrently measured, gaseous co-pollutant (CO), and then correlating its concentrations to particle concentrations. The total

number emission factors derived from this study agree well with previous on-road investigations. Road-level emissions are generally multi-modal, while grid-level emissions are distinctly mono-modal. Even with significantly different diesel truck fractions, the shapes and rates of grid-level emissions for Highway 405 and 710 are shown to be similar with conspicuous seasonal effects. The common modes shift from 40–100 nm in summer season to 10–20 nm in winter season. On-road fine-mode mass emission rates for trucks and non-trucks in around 133 and $21 \text{ mg km}^{-1} \text{vehicle}^{-1}$, respectively. We also observed distinct contrasts in the shapes of particle number and mass emission factor distributions that indicate that the effects of plume processing on particle number near roadways are much more profound than on particle mass.

Acknowledgment

KMZ, ASW and DAN would like to thank EPRI, NSF (Grants #CHE-0089136 & BES), UCD-CALTRANS Air Quality Project and the California Air Resources Board for supporting analysis and modeling of the data. C. Sioutas, W. Hinds and Y. Zhu would like to acknowledge support from the Southern California Particle Center and Supersite; US Environmental Protection Agency grants number R82735201, and CR8280260-01-0. We want to thank Kiettipong Jierranaitanakit, Bryan Jungers, Thomas Kear and Mihriban Sogutlugil at UC, Davis for their assistance in traffic analysis, and Dr. Tony Held for providing us the UCD 2001 model. KMZ and ASW appreciate the helpful discussion with Prof. Armistead G. Russell at Georgia Institute of Technology.

References

- Abu-Allaban, M., Coulomb, W., Gertler, A.W., Gillies, J., Pierson, W.R., Rogers, C.F., Sagebiel, J.C., Tarnay, L., 2002. Exhaust particle size distribution measurements at the Tuscarora Mountain tunnel. *Aerosol Science and Technology* 36 (6), 771–789.
- Benson, P.E., 1992. A Review of the development and application of the CALINE3 and CALINE4 models. *Atmospheric Environment Part B-Urban Atmosphere* 26 (3), 379–390.
- Cadle, S.H., Mulawa, P., Groblicki, P., Laroo, C., Ragazzi, R.A., Nelson, K., Gallagher, G., Zielinska, B., 2001. In-use light-duty gasoline vehicle particulate matter emissions on three driving cycles. *Environmental Science and Technology* 35 (1), 26–32.
- Gidhagen, L., Johansson, C., Strom, J., Kristensson, A., Swietlicki, E., Pirjola, L., Hansson, H.C., 2003. Model simulation of ultrafine particles inside a road tunnel. *Atmospheric Environment* 37 (15), 2023–2036.
- Gramotnev, G., Brown, R., Ristovski, Z., Hitchins, J., Morawska, L., 2003. Determination of average emission

- factors for vehicles on a busy road. *Atmospheric Environment* 37 (4), 465–474.
- Graskow, B.R., Kittelson, D.B., Abdul-Khalek, I.S., Ahmadi, M.R., Morris, J.E., 1998. Characterization of exhaust particulate emissions from a spark-ignition engine. SAE Paper No. 980528.
- Hall, D.E., Dickens, C.J., 2000. Measurement of the numbers of emitted gasoline particles: genuine or artifact? SAE Paper No. 2000-01-2957.
- Hall, D.E., Stradling, R.J., Rieckard, D.J., Heinze, P., Zemroch, P.J., Mann, N., Martini, G., Hagemann, R., Rantanen, L., Szendefi, J., 2000. Measurement of the number and size distribution of particle emissions from heavy duty engines. SAE Paper No. 2000-01-2000.
- Held, A.E., Chang, D.P.Y., Niemeier, D.A., 2001. Observations and model simulations of carbon monoxide emission factors from a California highway. *Journal of the Air and Waste Management Association* 51 (1), 121–132.
- Held, T., Chang, D.P.Y., Niemeier, D.A., 2003. UCD 2001: an improved model to simulate pollutant dispersion from roadways. *Atmospheric Environment* 37 (38), 5325–5336.
- Hlavinka, M.W., Bullin, J.A., 1988. Validation of mobile source emission estimates using mass balance techniques. *Journal of the Air Pollution Control Association* 38 (8), 1035–1039.
- Huang, C.-H., 1979. A theory of dispersion in turbulent shear-flow. *Atmospheric Environment* 13 (4), 453–463.
- Jamriska, M., Morawska, L., 2001. A model for determination of motor vehicle emission factors from on-road measurements with a focus on submicrometer particles. *Science of the Total Environment* 264 (3), 241–255.
- Janhäll, S., Åsa, M.J., Peter, M., Erik, A.S., Mattias, H., 2004. Size resolved traffic emission factors of submicrometer particles. *Atmospheric Environment* 38 (26), 4331–4340.
- Kean, A.J., Harley, R.A., Littlejohn, D., Kendall, G.R., 2003. Effects of vehicle speed and engine load on motor vehicle emissions. *Environmental Science and Technology* 37 (17), 3739–3746.
- Kirchstetter, T.W., Harley, R.A., Kreisberg, N.M., Stolzenburg, M.R., Hering, S.V., 1999. On-road measurement of fine particle and nitrogen oxide emissions from light- and heavy-duty motor vehicles. *Atmospheric Environment* 33 (18), 2955–2968.
- Kittelson, D.B., Watts, W.F., Johnson, J.P., 2004. Nanoparticle emissions on Minnesota highways. *Atmospheric Environment* 38 (1), 9–19.
- Kunzli, N., McConnell, R., Bates, D., Bastain, T., Hricko, A., Lurmann, F., Avol, E., Gilliland, F., Peters, J., 2003. Breathless in Los Angeles: the exhausting search for clean air. *American Journal of Public Health* 93 (9), 1494–1499.
- Maricq, M.M., Chase, R.E., Xu, N., Podsiadlik, D.H., 2002a. The effects of the catalytic converter and fuel sulfur level on motor vehicle particulate matter emissions: gasoline vehicles. *Environmental Science and Technology* 36 (2), 276–282.
- Maricq, M.M., Chase, R.E., Xu, N., Laing, P.M., 2002b. The effects of the catalytic converter and fuel sulfur level on motor vehicle particulate matter emissions: light duty diesel vehicles. *Environmental Science and Technology* 36 (2), 283–289.
- McGaughey, G.R., Desai, N.R., Allen, D.T., Seila, R.L., Lonneman, W.A., Fraser, M.P., Harley, R.A., Pollack, A.K., Ivy, J.M., Price, J.H., 2004. Analysis of motor vehicle emissions in a Houston tunnel during the Texas Air Quality Study 2000. *Atmospheric Environment* 38 (20), 3363–3372.
- Mulholland, M., Seinfeld, J.H., 1995. Inverse air pollution modelling of urban-scale carbon monoxide emissions. *Atmospheric Environment* 29 (4), 497–516.
- Palmgren, Finn., Ruwim, Berkowicz., Alexander, Ziv., Ole, Hertel., 1999. Actual car fleet emissions estimated from urban air quality measurements and street pollution models. *The Science of the Total Environment* 235 (1–3), 101–109.
- Park, K., Cao, F., Kittelson, D.B., McMurry, P.H., 2003. Relationship between particle mass and mobility for diesel exhaust particles. *Environmental Science and Technology* 37 (3), 577–583.
- Rieckard, D.J., Bateman, J.R., Kwo, Y.K., McAughey, J.J., Dicken, C.J., 1996. Exhaust particulate size distribution, vehicle and fuel influences in light duty vehicles. SAE Paper No. 961980.
- Stull, R.B., 1988. *An Introduction to Boundary Layer Meteorology*. Kluwer Academic Publishers, Boston.
- Sawyer, R.F., Harley, R.A., Cadle, S.H., Norbeck, J.M., Slott, R., Bravo, H.A., 2000. Mobile sources critical review: 1998 NARSTO assessment. *Atmospheric Environment* 34 (12–14), 2161–2181.
- Singer, B.C., Harley, R.A., 1996. A fuel-based motor vehicle emission inventory. *Journal of the Air and Waste Management Association* 46 (6), 581–593.
- Singer, B.C., Harley, R.A., 2000. A fuel-based inventory of motor vehicle exhaust emissions in the Los Angeles area during summer 1997. *Atmospheric Environment* 34 (11), 1783–1795.
- Zhang, K.M., Wexler, A.S., 2002. Modeling the number distributions of urban and regional aerosols: theoretical foundations. *Atmospheric Environment* 36 (11), 1863–1874.
- Zhang, K.M., Wexler, A.S., 2004. Evolution of particle number distribution near roadways Part I: analysis of aerosol dynamics and its implications for engine emission measurement. *Atmospheric Environment* 38 (38), 6643–6653.
- Zhang, K.M., Wexler, A.S., Zhu, Y.F., Hinds, W.C., Sioutas, C., 2004. Evolution of particle number distributions near roadways Part II: the road-to-ambient process. *Atmospheric Environment* 38 (38), 6655–6665.
- Zhu, Y., Hinds, W.C., Kim, S., Sioutas, C., 2002a. Concentration and size distribution of ultrafine particles near a major highway. *Journal of the Air and Waste Management Association* 52, 1032–1042.
- Zhu, Y., Hinds, W.C., Kim, S., Shen, S., Sioutas, C., 2002b. Study of ultrafine particles near a major highway with heavy-duty diesel traffic. *Atmospheric Environment* 36 (27), 4323–4335.